Preparation and Characterization of Different Phases of Aluminum Trifluoride

ARTICLE *in* CHEMISTRY OF MATERIALS · MARCH 2000

Impact Factor: 8.35 · DOI: 10.1021/cm991195g

7 AUTHORS, INCLUDING:

Francesc Medina
Universitat Rovira i Virgili
138 PUBLICATIONS **2,464** CITATIONS
SEE PROFILE

Francesc Gispert Guirado
Universitat Rovira i Virgili
59 PUBLICATIONS **416** CITATIONS
SEE PROFILE

Preparation and Characterization of Different Phases of Aluminum Trifluoride

C. Alonso,[†] A. Morato,[†] F. Medina,*[,†] F. Guirado,[‡] Y. Cesteros,[§] P. Salagre,[§] and J. E. Sueiras[†]

Departament d'Enginyeria Química, ETSEQ; Servei de Recursos Científics; and Facultad de Química, Universitat Rovira i Virgili, Pl. Imperial Tarraco 1, 43005 Tarragona, Spain

R. Terrado and A. Giralt

Kal y Sol Iberia S.A., Pol. Industrial "Can Roca", C/San Martín s/n, 08107 Martorelles, Barcelona, Spain

Received December 20, 1999

Several phases (α, ϵ_2, and γ) of aluminum fluoride were prepared from precursors such as NH_4AlF_4, $(NH_4)_3AlF_6$, and β-$AlF_3 \cdot 3H_2O$ using various synthetic strategies. The precursors and the aluminum fluoride phases obtained were characterized by X-ray diffraction (XRD), X-ray fluorescence, scanning electron microscopy (SEM), and infrared spectra (FT-IR). The structural evolution of the precursors to the different phases of aluminum fluoride during thermal treatment was studied by dynamic XRD experiments, differential scanning calorimetry (DSC), and thermogravimetric analysis (TGA). α- and γ-AlF_3 phases were obtained with high BET surface areas (>120 and 30 m^2/g, respectively). These aluminum fluorides with high BET areas are of potential interest as supports or catalysts in hydrodechlorination and fluorination reactions.

Introduction

Complex fluorides with various interesting structures have been extensively studied for their particular physical properties such as their piezoelectric characteristics,[1−2] photoluminescence,[3] ionic conductivity,[4] and nonmagnetic insulation.[5] Recent studies have also demonstrated that several phases of aluminum fluorides are important inorganic materials, since they can be used both as commodity chemicals (in the aluminum industry) and as catalysts for the new, ozone-friendly alternatives to chlorofluorocarbons.[6−7]

Two phases of AlF_3 are well-characterized (α and β), and reliable synthetic and structural data are available. In both cases, the structures are built of octahedral [AlF_6] units where all the fluoride ions are corner-shared.[8−9] α-AlF_3 was prepared by passing gaseous hydrogen fluoride over anhydrous $AlCl_3$ at 1073 K,[10] and crystallizing with a rhombohedral structure and space group *R*3*c*.[11] β-AlF_3 was obtained by dehydrating α-$AlF_3 \cdot 3H_2O$ at 723 K.[8] The crystal structure of β-AlF_3 is orthorhombic with space group *Cmcm*. The metastable form β-AlF_3 irreversibly transforms to stable α-AlF_3 when heated at 773 K.

However, the literature is full of other metastable phases (γ, t, ϵ) which may represent either impure materials or mixtures of the better-characterized phases.[7] γ-AlF_3 was prepared from the thermal decomposition of the ammonium hexafluoroaluminate.[10] $(NH_4)_3AlF_6$ decomposed on heating with an initial loss of 2 mol of ammonium fluoride to form ammonium tetrafluoroaluminate at 443 K. Further heating resulted in the gradual loss of ammonium fluoride. The final product was γ-AlF_3. When γ-AlF_3 was heated to 983−993 K, an irreversible transition to α-AlF_3 occurred. The crystal structure of γ-AlF_3 is tetragonal.[10]

Moreover, t-AlF_3 was first encountered as a product of the crystallization of an amorphous material, $AlF_3 \cdot xH_2O$ ($x < 0.5$), synthesized by dehydration under high vacuum of $AlF_3 \cdot 9H_2O$.[12] t-AlF_3 was also obtained by dehydration of $[(CH_3)_4N]AlF_4 \cdot H_2O$ under vacuum at 723 K. The space group of t-AlF_3 is *P*4/*nmm*, and it is built of octahedral [AlF_6] units.[12]

ϵ_1-AlF_3, which corresponds to $AlF_3 \cdot 1.5H_2O$, was obtained by evaporating an aqueous hydrofluoric acid

[†] Departament d'Enginyeria Química.
[‡] Servei de Recursos Científics.
[§] Facultad de Química.

(1) Eibschutz, M.; Guggenheim, H. J. *Solid State Commun.* **1998**, *6*, 737.
(2) Eibschutz, M.; *Phys. Lett. A* **1969**, 409.
(3) Sardar, D. K.; Sibley, W. A.; Aicala, R. *J. Lumin.* **1982**, *27*, 401.
(4) West, A. R. *Solid State Chemistry and Its Applications*; Wiley: New York, 1984.
(5) Heaton, R. A.; Chun, C. L. *Phys Rev. B.* **1982**, *25*, 3538.
(6) Herron, N.; Thorn, D.; Harlow, R.; Davidson, F. *Chem. Mater.* **1995**, *7*, 75.
(7) Herron, N.; Farneth, W. *Adv. Mater.* **1996**, *8*, 959.
(8) Le Bail, A.; Jacoboni, C.; Leblac, M.; DePape, H.; Duroy, H.; Fourquet, J. L. *J. Solid State Chem.* **1988**, *77*, 96.
(9) Hoppe, R.; Kissel, D. *J. Fluorine Chem.* **1984**, *24*, 327.
(10) Shinn, D.; Crocket, D.; Haendler, H. *Inorg. Chem.* **1966**, *5*, 1927.
(11) Hanic, F.; Stempelova, D. *Theory and Structure of Complex Compounds*; Jezowska-Trzebiatowska, B., Ed.; Macmillan: New York, 1964.
(12) Le Bail, A.; Fourquet, J. L.; Bentrup, U. *J. Solid State Chem.* **1992**, *100*, 151.

10.1021/cm991195g CCC: $19.00
Published on Web 03/21/2000

solution of AlF_3 under vacuum to dryness at a temperature from 303 to 393 K. ϵ_1-AlF_3 gradually changed to ϵ_2-AlF_3 ($AlF_3 \cdot 0.5H_2O$) when heated above 393 K. In addition, ϵ_2-AlF_3 transformed to ϵ_3-AlF_3 (AlF_3) at a temperature above 453 K. ϵ_3-AlF_3 also converted to α-AlF_3 when heated above 773 K.[13]

The above AlF_3 phases were synthesized by using aqueous chemistry and, if necessary, operated using excess fluoride to avoid contaminating the materials with hydroxide or oxide phases.

Other phases of AlF_3 (η, θ, κ) were prepared by applying a nonaqueous soft chemistry. η-AlF_3 and θ-AlF_3 were obtained using $HAlF_4$ as precursor. The η-AlF_3 crystal system is cubic, and the space group is $Fd3m$. The θ-AlF_3 crystal system is tetragonal, and its space group is $P4/nmm$. κ-AlF_3 was synthesized by heating β-NH_4AlF_4 to 723 K. Both precursors, $HAlF_4$ and β-NH_4AlF_4, were obtained from (pyridine−H)−AlF_4.[14−15]

It has been reported recently that aluminum fluoride phases such as η, θ, κ, and β have interesting catalytic properties for fluorination reactions of chlorofluorocarbon compounds (CFCs). The activity and selectivity depend very much on its structural phase and surface area.[7,16]

This study aims to synthesize α-, γ-, and ϵ_2-AlF_3 of high surface areas by using different precursors and synthetic strategies. This work may render a novel contribution as far as AlF_3's with very high surface areas are successfully obtained by any of those synthetic strategies. The evolution of metastable phases and the transformation of the precursors under calcination conditions are also systematically studied.

Experimental Section

Preparation of the Precursors. NH_4AlF_4, $(NH_4)_3AlF_6$, and β-$AlF_3 \cdot 3H_2O$ were the precursors that were thermally transformed into the different AlF_3 phases. Different routes of synthesis were performed, and these are described below.

Preparation of NH_4AlF_4. Ammonium tetrafluoroaluminate (NH_4AlF_4) was prepared by the following procedures.

Procedure 1. Precursor P1 was obtained by coprecipitation of two aqueous solutions, $Al(NO)_3 \cdot 9H_2O$ (1 M) and NH_4F (1 M), in a molar ratio of 1:4, respectively. The two solutions were mixed in a Teflon reaction vessel initially containing distilled water. The precipitation process was performed dropwise under continuous magnetic stirring. Then, an aging process was carried out overnight at 333 K. The precipitate was filtered, washed with ethanol, and dried at 373 K for 24 h.

Procedure 2. Precursor P2 was synthesized following the same procedure as precursor P1, but no aging process was carried out.

Procedure 3. An appropriate amount of a solution of $Al(NO)_3 \cdot 9H_2O$ (1 M) was precipitated with an aqueous solution of NH_3 (1 M) at room temperature and constant pH = 10. The gel was filtered and washed with distilled water to eliminate the ammonia excess. The gel was then suspended in a Teflon vessel in 25 mL of distilled water under magnetic stirring. An appropriate amount of an aqueous solution of ammonium fluoride (1 M) was added dropwise. The sample was then stirred and heated overnight (333K). The solid that formed (precursor P3) was filtered, washed with ethanol and dried at 373 K for 24 h.

Procedure 4. Stoichiometric amounts of two aqueous solutions of $Al(NO)_3 \cdot 9H_2O$ (1 M) and NH_4F (1 M) were added drop by drop to a Teflon reaction vessel containing 50 mL of ethanol. The gel formed (precursor P4) was filtered, washed with ethanol, and dried at 373 K for 24 h.

Procedure 5. Precursor P5 was prepared by adding an appropriate amount of an aqueous solution of ammonium fluoride (1 M) dropwise to a Teflon reaction vessel containing 2 g of γ-alumina (Norton, NL00791) suspended in 25 mL of distilled water. The process was performed under continuous magnetic stirring and heated overnight at 333 K. The gel was filtered, washed with ethanol, and dried at 373 K for 24 h.

Preparation of $(NH_4)_3AlF_6$. Aluminum hexafluoroaluminate $(NH_4)_3AlF_6$ was prepared following procedures 1, 3, and 5 mentioned above. An excess of ammonium fluoride was used to avoid the formation of side phases. The precursors obtained were labeled P6, P7, and P8, respectively.

Preparation of β-$AlF_3 \cdot 3H_2O$. β-$AlF_3 \cdot 3H_2O$ was synthesized in the following ways.

Procedure 9. An appropriate amount of a solution of $Al(NO)_3 \cdot 9H_2O$ (1 M) was precipitated with an aqueous solution of NH_3 (1 M) at room temperature and constant pH = 10. The gel was filtered and washed with distilled water to eliminate the ammonia excess. It was then suspended in 25 mL of distilled water in a Teflon vessel under magnetic stirring. An appropriate amount of hydrofluoric acid was added drop by drop until pH = 1 was reached. The sample was stirred and heated overnight at 333 K. The product (precursor P9) was then filtered, washed with water and ethanol, and dried at 373 K for 24 h.

Procedure 10. γ-Alumina(2 g, Norton, NL00791) was suspended in 25 mL of distilled water in a Teflon reaction vessel. An appropriate amount of hydrofluoric acid was added dropwise until acid pH was reached. The sample was heated at 333 K and stirred overnight. The precipitate formed (precursor P10) was filtered, washed with water and ethanol, and dried at 373 K for 24 h.

Procedure 11. γ-Alumina (2 g) was impregnated with concentrated hydrofluoric acid. The sample was dried at 373 K for 24 h. The solid obtained was labeled precursor P11.

Procedure 12. β-$AlF_3 \cdot 3H_2O$ from Rhône Poulenc was used as precursor P12.

Preparation of Aluminum Fluoride Phases. The different phases of aluminum fluoride were prepared by calcination of the different precursors described above. Precursors P1−P8 were heated (2 K/min) to 673 K under an argon-flowing atmosphere and held at this temperature for 4 h. The samples obtained by calcination were labeled S1−S8, respectively.

Precursors P9−P12 were heated (2 K/min) to 623 K under an argon-flowing atmosphere and held at this temperature for 4 h. The samples were labeled S9−S12, respectively.

Precursor P12 was also heated at 2 K/min up to 453 K under an argon-flowing atmosphere and held at this temperature for 4 h, and the sample obtained was labeled S13.

X-ray Diffraction. XRD measurements were made using a Siemens D5000 diffractometer (Bragg−Brentano parafocusing geometry and vertical $\theta-\theta$ goniometer) fitted with a curved graphite diffracted-beam monochromator, incident and diffracted-beam Soller slits, a 0.03° receiving slit, and a scintillation counter as detector. The angular 2θ diffraction range was between 5 and 70°. The data were collected with an angular step of 0.05° at 3 s per step. Cu Kα radiation was obtained from a copper X-ray tube operated at 40 kV and 30 mA. The patterns were compared to the X-ray powder files to confirm phase identities. The patterns for $(NH_4)_3AlF_6$, NH_4AlF_4, α-AlF_3, β-AlF_3, γ-AlF_3, and β-$AlF_3 \cdot 3H_2O$ were obtained from the files of the Joint Committee for Powder Diffraction Sources (JCPDS). The patterns for ϵ_1-AlF_3, ϵ_2-AlF_3, and ϵ_3-AlF_3 were obtained from U.S. Patent No. 3,929,415.[13]

Infrared Spectra (FT-IR). The infrared spectra (FT-IR) were recorded with a Nicolet 5ZDX spectrometer in the 4000−400 cm^{-1} wavenumber range using pressed KBr pellets.

(13) Wada, H.; Kawakami, Y.; Kamihigoshi, T. U.S. Patent 3 929 415, 1975.

(14) Harlow, R.; Herron, N. U.S. Patent 5 417 954 1995.

(15) Herron, N.; Thorn, D.; Harlow, R.; Davidson, F. *J. Am. Chem. Soc.* **1993**, *115*, 3028.

(16) Kemnitz, E.; Kohne, A.; Lieske, E. *J. Fluorine Chem.* **1997**, *81*, 197.

Table 1. Phases Detected by XRD and BET Areas of the Precursors and the Samples

precursor	precursor crystal phase	calcinat. temp (K)	sample	sample crystal phase	sample BET area (m^2/g)
P1	NH_4AlF_4	673	S1	γ-AlF_3	26.2
P2	NH_4AlF_4	673	S2	γ-AlF_3	25.3
P3	NH_4AlF_4	673	S3	γ-AlF_3	30.3
P4	NH_4AlF_4	673	S4	γ-AlF_3	<1.0
P5	NH_4AlF_4	673	S5	γ-AlF_3	24.7
P6	$(NH_4)_3AlF_6$	673	S6	γ-AlF_3	16.6
P7	$(NH_4)_3AlF_6$	673	S7	γ-AlF_3	20.5
P8	$(NH_4)_3AlF_6$	673	S8	γ-AlF_3	27.8
P9	β-$AlF_3{\cdot}3H_2O$	623	S9	α-AlF_3	71.4
P10	β-$AlF_3{\cdot}3H_2O$	623	S10	α-AlF_3	123.5
P11	β-$AlF_3{\cdot}3H_2O$	623	S11	α-AlF_3	110.6
P12	β-$AlF_3{\cdot}3H_2O$	623	S12	α-AlF_3	101.3

Thermogravimetric Analysis. Thermogravimetric analyses were carried out in a Perkin-Elmer TGA 7 microbalance with an accuracy of 1 mg, equipped with a 273−1273 K programmable temperature furnace. The samples were heated from 373 to 1073 K at a rate of 10 K/min.

X-ray Fluorescence. X-ray fluorescence analysis were made with a Philips EM 301 microscopy equipped with an electron probe microanalysis (EPMA), CAMECA Camebax SX-50, and operating at acceleration voltages = 35−45 kV. The molar ratios of F, Al, N, and O of the samples were obtained.

Temperature XRD. XRD measurements were registered using a Siemens D5000 diffractometer (Bragg−Brentano parafocusing geometry and vertical $\theta-\theta$ goniometer) equipped with an Anton−Paar HTK10 platinum ribbon heating stage. The angular 2θ diffraction range was between 10 and 70° and the measuring time per degree was 60 s. Ni-filtered Cu Kα radiation (30 mA, 40 kV) and a Braun position sensitive detector (PSD) were used. The patterns were collected from 373 to 1223 K and at a heating rate of 2 K/min. A static air atmosphere was used throughout the measurement.

Differential Scanning Calorimetry (DSC). The existence of phase transitions was checked by differential scanning calorimetry. Experiments were performed using a Setaram (TG−DTA−DSC) microbalance. The samples were heated in a sealed alumina crucible at a temperature range from 373 to 1173 K at a heating rate of 10 K/min in an argon-flowing atmosphere.

Scanning Electron Microscopy (SEM). Scanning electron micrographs were obtained in a JEOL JSM-35C microscope operating at acceleration voltages of 15−25 kV, working distances of 8−19 mm, and magnification values up to 150 000×.

BET Areas. BET surface areas were calculated from the nitrogen adsorption isotherms at 77 K by using Micromeretics ASAP 2000 surface analyzer and a value of 0.164 nm^2 for cross section of the nitrogen molecule.

Results and Discussion

X-ray Diffraction. Table 1 summarizes the crystalline phases detected by conventional X-ray diffraction for the precursors and the samples obtained from their calcination. The powder diffraction patterns of the precursors reveal that pure NH_4AlF_4 is detected in the precursors P1−P5 and pure $(NH_4)_3AlF_6$ is obtained in precursors P6−P8. Calcination of the precursors P1−P8 at 673 K yield pure γ-AlF_3 (samples S1−S8).

The crystal structure obtained in the precursors P9−P12 is β-$AlF_3{\cdot}3H_2O$. Pure α-AlF_3 is obtained by calcination of the precursors P9−P12 at temperatures around 623 K (samples S9−S12). When precursors P9−P12 are calcined at temperatures below 453 K, the ϵ_2-AlF_3 phase is obtained.

Infrared Spectra (FT-IR). The infrared spectra of precursors and calcined samples are shown in Figures1 and 2, respectively. The trends for precursors P1−P5 are similar. The frequency bands at 3250, 3130, 2898, 1800, and 1447 cm^{-1} are assigned to ammonium vibrations and correspond to the characteristic IR spectrum of NH_4AlF_4.[10,18] The broad band near 3250 cm^{-1} is typical of the asymmetric stretching of ammonium ions in the solid state.[17] The frequency band near 1800 cm^{-1} is assigned to hydrogen bonding.[18] Moreover, the two bands between 600 and 700 cm^{-1} are assigned to aluminum fluoride vibrations. This splitting is attributed to two perfect AlF_6 octahedra with relatively different orientations.[19,20] However, the band at 1654 cm^{-1} is attributed to the presence of water in the sample (probably due to moisture).

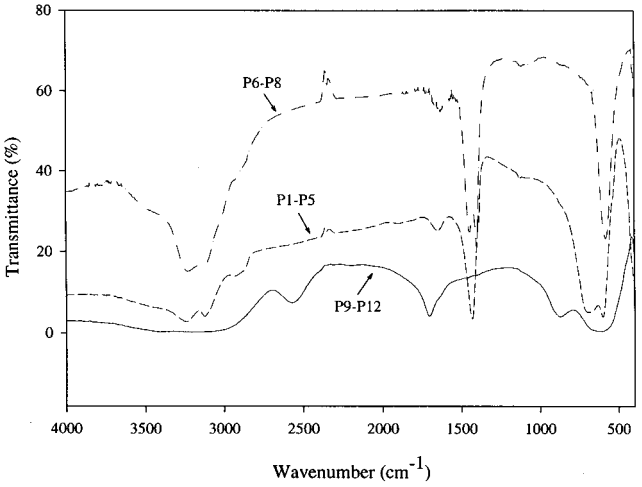

Figure 1. Infrared spectra of precursors P1−P5, P6−P8, and P9−P12.

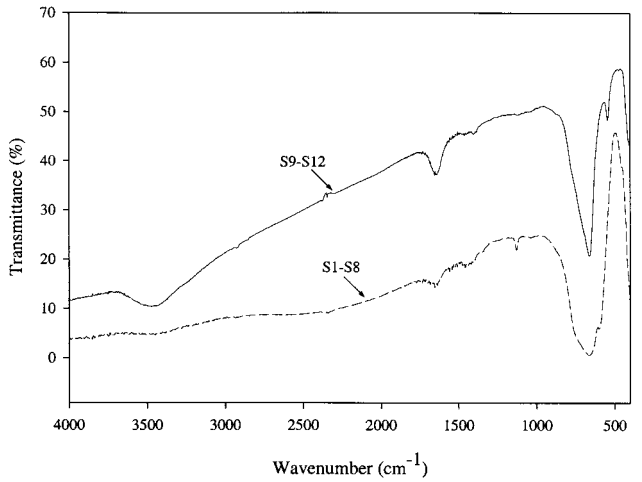

Figure 2. Infrared spectra of samples S1−S8 and S9−S12.

The presence of the frequency bands at 3213, 3123, and 1431 cm^{-1} in the infrared spectra of precursors P6−P8 is characteristic of $(NH_4)_3AlF_6$, and these bands are attributed to ammonium vibrations. The splitting of the band at around 1440 cm^{-1} is indicative of two nonequivalent kinds of ammonium groups,[6] and the band at 586 cm^{-1} is attributed to the stretching vibrations of AlF_6 groups.[10]

(17) White, M.; Shi, H.; Leiper, J. *J. Fluorine Chem.* **1993**, *62*, 211.
(18) Waddington, T. *J. Chem. Soc.* **1958**, 4340.
(19) Peacock, R.; Sharpe, D. *J. Chem. Soc.* **1959**, 2762.
(20) Bulou, A.; Leblé, A.; Hewat, A. W. *Mater. Res. Bull.* **1982**, *17*, 391.

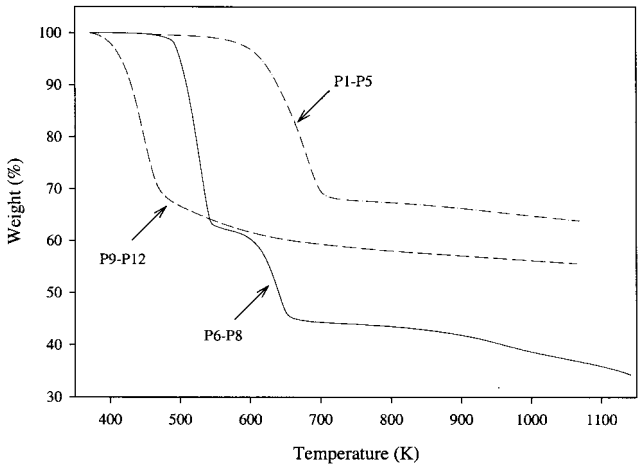

Figure 3. Thermogravimetric analysis of precursors P1−P5, P6−P8, and P9−P12.

The IR spectra of precursors P9−P12 are characteristic of β-$AlF_3 \cdot 3H_2O$.[21]

The bands at 687 and 541 cm^{-1} in the infrared spectra of samples S1−S8 and the bands at 687 and 534 cm^{-1} of samples S9−S12 (Figure 2) are attributed to the vibrations of the AlF_6 octahedra in the γ- and α-AlF_3's, respectively.

Thermogravimetric Analysis. The results of the thermogravimetric analysis of precursors P1−P4 (NH_4AlF_4) (Figure 3) show a single weight loss of 30.5% between 623 and 683 K, which corresponds to the loss of 1 mol of NH_4F to form γ-AlF_3. So, thermogravimetric analysis shows that mainly pure NH_4AlF_4 phase is obtained from procedures P1−P5, in agreement with the XRD results.

The TG curve of precursors P6−P8 ($(NH_4)_3AlF_6$) (Figure 3), indicates two weight losses. The first weight loss (around 37.9%), performed below 600 K, can be assigned to the loss of 2 mol of ammonium fluoride to form NH_4AlF_4 (the stoichiometric value is 38%). The second weight loss (around 18.9%), below 700 K, can be attributed to the loss of 1 mol of ammonium fluoride to form γ-AlF_3 (the stoichiometric value is 19%). However, there is a new weight loss of around 8% between 800 and 1000 K. The nature of the gases released during the thermal treatment of precursors P6−P8 were monitored by mass spectrometry, and the following masses were detected: 18−16 (H_2O), 17−14 (NH_3), 19−20 (HF), and 19−38 (F_2). The main species detected by mass spectrometry during the decomposition process, at lower calcination temperatures (<600 K) are NH_3, HF, F_2, and traces of water (due to sample moisture). These species are also detected at higher calcination temperatures (>800 K). Ammonium fluoride is also precipitated in the cold zone of the equipment. The NH_3, HF, F_2, and traces of H_2O detected at high temperatures (>800 K) could be related to the presence of some aluminum oxihydroxifluoride phases or with the presence of a nonstoichiometric $(NH_4)_{1+x}AlF_{4+x}$ compound obtained during the decomposition process of $(NH_4)_3AlF_6$, due to some incorporation of ammonium fluoride inside the structure of NH_4AlF_4. So, the weight losses detected during the calcination process of the P1−P5 and P6−P8 precursors confirm that mainly pure NH_4AlF_4 and $(NH_4)_3AlF_6$ phases, respectively, are obtained following the experimental procedures described in the Experimental Section. This agrees with the XRD results and X-ray fluorescence analysis that are mentioned below. It is important to mention that an excess of ammonium fluoride is required for the preparation of $(NH_4)_3AlF_6$, from our experimental procedures to avoid the formation of a mixture of NH_4AlF_4 and $(NH_4)_3AlF_6$ phases.

(21) Nyquist, R. A.; Kagel, R. O. *Infrared Spectra of Inorganic Compounds*; Academic Press: London, 1971.

Table 2: Al, N, O, and F Atomic Percentage of Precursors and Samples by X-ray Fluorescence

compound	% Al	% N	% O	% F
P1−P5	16.58	16.75	0.16	66.51
P6−P8	9.85	30.07	0.29	59.79
P9−P12	13.71		45.26	41.03
S1−S5	24.27	2.55	0.30	72.88
S6−S8	22.75	4.50	0.28	72.47
S9−S12	24.05		4.85	71.10

Figure 3 shows the characteristic TG curve of precursor P9 (β-$AlF_3 \cdot 3H_2O$). Precursors P10−P12 show similar behavior. The weight loss is a two-step process. The first (below 473 K) is around 32% and corresponds to the formation of $AlF_3 \cdot 0.5H_2O$ (ϵ_2-AlF_3). The second step (above 500 K) shows a slow weight loss slightly greater than the one corresponding to the removal of 0.5 mol of water to form α-AlF_3. This could be attributed to the presence of other side phases that are not detected by XRD. Therefore, mainly β-$AlF_3 \cdot 3H_2O$ is obtained (precursors P9−P12) following our experimental procedures.

X-ray Fluorescence. To obtain more information about the chemical composition of our precursors, and the purity of the phases obtained after their calcination, X-ray fluorescence analysis were performed. More than 20 analysis of F, Al, N, and O were performed for each sample. The average atomic percentages of these elements are shown in Table 2. Precursors P1−P5 show that a practically pure NH_4AlF_4 phase is obtained. The slight amount of oxygen could be attributed to sample moisture. Furthermore, Table 2 shows that pure $(NH_4)_3AlF_6$ phase is obtained for P6−P8 precursors from our experimental procedures. The oxygen detected could also be attributed to sample moisture. The elemental analysis of the precursors P9−P12 revealed that mainly pure β-$AlF_3 \cdot 3H_2O$ is obtained. These results are in agreement with the conventional X-ray diffraction and thermogravimetric analysis.

Table 2 also shows the average atomic percentages of Al, O, N, and F of the samples S1−S12 obtained by calcination of the precursors P1−P12, respectively. The results obtained for samples S1−S8 reveal the presence of a slight amount of nitrogen, probably indicating that the calcination process was not totally achieved. Besides, traces of oxygen, probably due to moisture, are also detected in the samples. Samples S9−S12 show higher amounts of oxygen than those of S1−S8 samples: probably all the water was removed during the calcination process. So, we can conclude that pure NH_4AlF_4, $(NH_4)_3AlF_6$, β-$AlF_3 \cdot 3H_2O$, and alumnium fluoride phases are obtained with the procedures described above.

Temperature X-ray Diffraction. To detect the appearance of some metastable phase and to study the transition of precursors during the calcination process more accurately, several experiments were performed

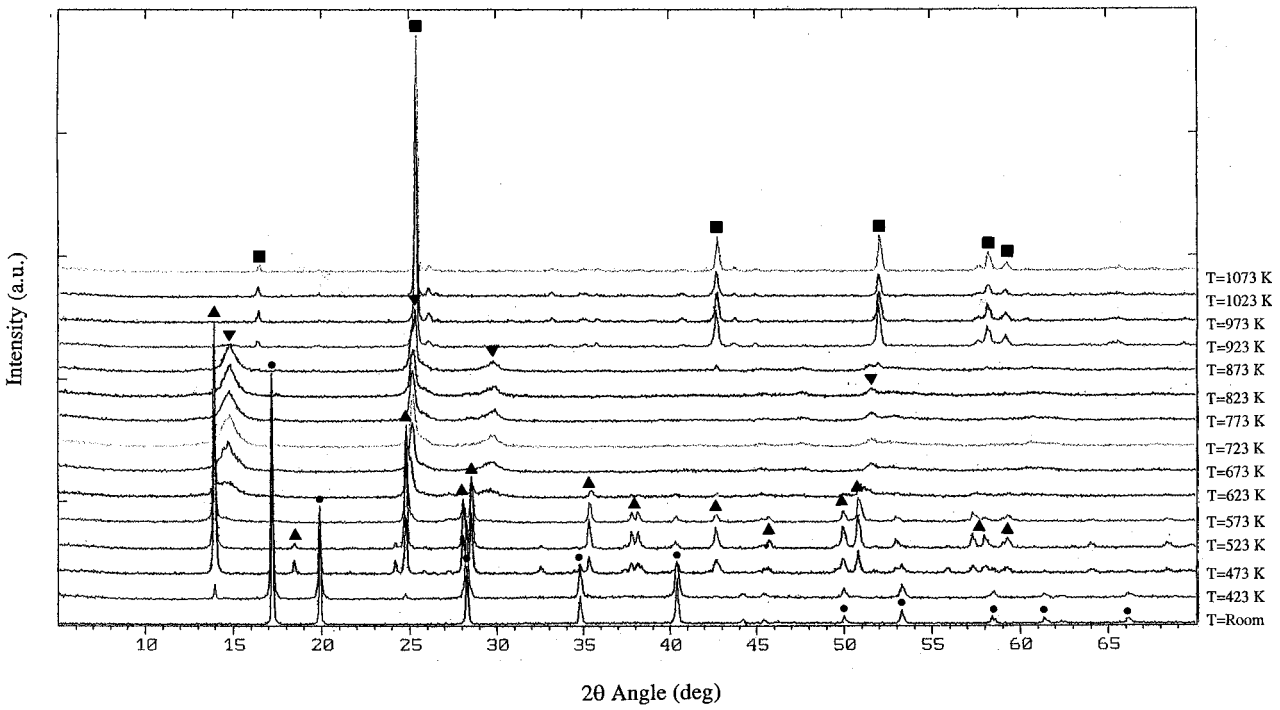

Figure 4. Temperature X-ray diffraction analysis of precursors P6−P8: ●, $(NH_4)_3AlF_6$; ▲, NH_4AlF_4; ▼, γ-AlF_3; ■, α-AlF_3.

Table 3: Cell Parameters (in Å) Obtained from Profile Analysis for $(NH_4)_3AlF_6$, NH_4AlF_4, γ-AlF_3 and α-AlF_3

	$(NH_4)_3AlF_6$	NH_4AlF_4		γ-AlF_3		α-AlF_3
temp (K)	*a, b, c*	*a, b*	*c*	*a, b*	*c*	*a, b, c*
423	5.1507	3.5941	6.3496			
473	5.1489	3.5926	6.3436			
523		3.5916	6.3495			
573		3.5896	6.3551	3.5518	6.1177	
623		3.5812	6.3414	3.5641	6.0726	
673				3.5422	6.0257	
723				3.5369	6.0066	
773				3.5393	6.0066	
823				3.5365	5.9881	
873				3.5543	5.9828	3.5279
923						3.5188
973						3.5162
1023						3.5205
1073						3.5131

using a high-temperature chamber attached to the X-ray diffractometer. Temperature XRD measurements of precursors P6−P8, $(NH_4)_3AlF_6$, between 373 K up to 1073 K reveal (Figure 4) that $(NH_4)_3AlF_6$ is the only phase detected at temperatures below 423 K (Figure 4). At temperatures between 423 and 473 K, there is a coexistence of $(NH_4)_3AlF_6$ and NH_4AlF_4. Pure NH_4AlF_4 is obtained at temperatures between 523 and 573 K. At these temperatures, the typical diffraction lines of NH_4AlF_4 practically remain constant during the initial loss of ammonium fluoride, prior to the detection of γ-AlF_3 phase (see Table 3). These results suggest that, at temperatures below 573, the crystal structure of NH_4AlF_4 is maintained during the initial loss of ammonium fluoride indicating the formation of a nonstoichiometric compound of variable composition, such as $(NH_4)_{1-x}AlF_{4-x}$.[10] When the γ-AlF_3 phase appears, the diffraction lines of NH_4AlF_4 are shifted to higher 2θ degrees (around 623 K), indicating that the loss of ammonium fluoride produces a decrease of the cell parameters (see Table 4). γ-AlF_3 is the only phase detected at temperatures between 673 and 823 K, and γ-AlF_3 and α-AlF_3 coexist at temperatures of around 873 K. When the temperature increases up to 923 K, γ-AlF_3 is totally transformed into α-AlF_3. The $(NH_4)_3AlF_6$, NH_4AlF_4, γ-AlF_3, and α-AlF_3 crystallite sizes (calculated from the Scherrer equation) of the samples are around 78 and 75 nm for the $(NH_4)_3AlF_6$ and NH_4AlF_4 phases, respectively. In addition, the crystallite sizes for γ-AlF_3 are between 5 and 10 nm, and around 78 nm for α-AlF_3. Therefore, $(NH_4)_3AlF_6$, NH_4AlF_4, and α-AlF_3 phases show similar crystallite sizes that are much higher than those for the γ-AlF_3 phase. Temperature X-ray measurements of precursors P1−P5 (NH_4AlF_4) (not shown) show behavior similar to that of P6−P8 ($(NH_4)_3AlF_6$) after their loss of 2 mol of ammonium fluoride to form NH_4AlF_4.

Table 4. Cell Parameters (in Å) Obtained from Profile Analysis for β-$AlF_3{\cdot}3H_2O$

	β-$AlF_3{\cdot}3H_2O$	
temp (K)	*a, b*	*c*
373	7.7318	3.6498
393	7.7345	3.6484
413	7.7423	3.6462

Furthermore, temperature X-ray measurements of precursors P9−P12 show (Figure 5) that β-$AlF_3{\cdot}3H_2O$ is the phase present at 373 K. When the temperature is raised to between 393 and 413 K, a decrease of the intensity of β-AlF_3 $3H_2O$ phase is detected in the XRD patterns. ϵ_2-AlF_3 is the structure with poor crystallinity detected at temperatures around 473 K that corresponds to the empirical formula $AlF_3{\cdot}0.5H_2O$. On the other hand, α-AlF_3 is the crystal structure obtained at temperatures above 573 K. The cell parameters were calculated by fitting the XRD profile in a temperature range between 373 and 413 K to study the transformations of the β-$AlF_3{\cdot}3H_2O$ cell with temperature prior to its complete transformation to α-AlF_3 (see Table 4). The results show that parameters *a* and *b* increase as a result of the cell expansion induced by the effect of

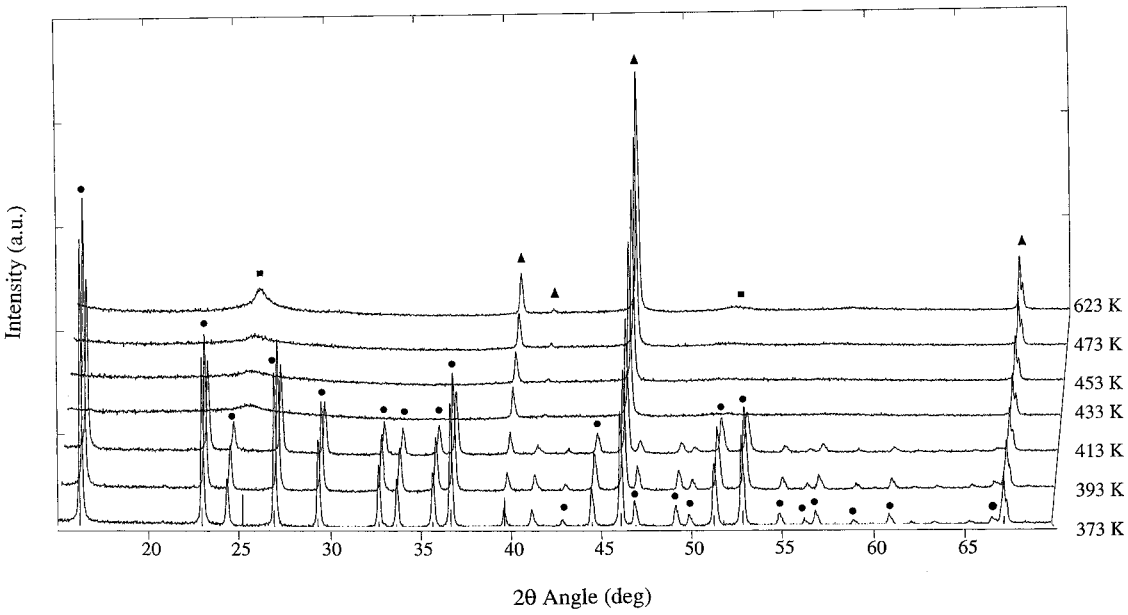

Figure 5. Temperature X-ray diffraction analysis of precursors P9−P12: ●, β-$AlF_3 \cdot 3H_2O$; ▲, platinum; ■, α-AlF_3.

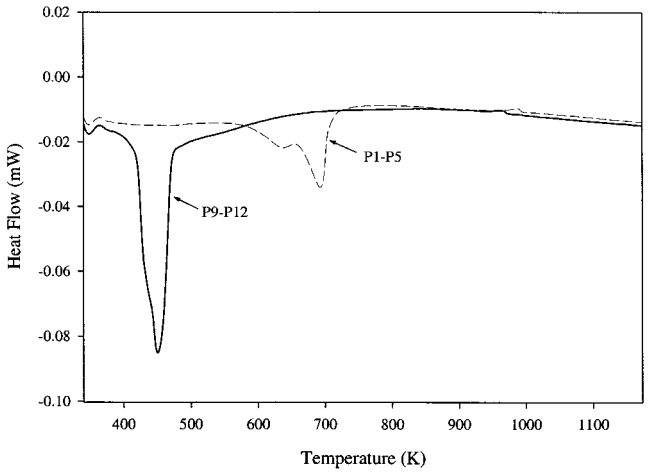

Figure 6. Differential scanning calorimetry of precursors P1−P5 and P9−P12.

temperature. On the other hand, parameter *c* decreases when the temperature increases because the effect of the loss of water is higher than the effect of the cell expansion induced by the effect of the temperature.

Differential Scanning Calorimetry (DSC). DSC experiments on precursors P1−P5 (NH_4AlF_4) show three endothermic peaks (Figure 6). The first one, at 373 K, corresponds to the loss of water (probably due to sample moisture). The second and third peaks, between 570 and 730 K, represent the transformation of NH_4AlF_4 to γ-AlF_3. The second peak may be attributed to the formation of a nonstoichiometric intermediate during the initial loss of ammonium fluoride. The formation of this intermediate can be seen on the TG curve (Figure 7), which shows a shoulder in their derivative curve around 623 K. The formation of this nonstoichiometric intermediate has been previously reported by Shin et al.[10] The third peak corresponds with the total decomposition of this intermediate into γ-AlF_3. Moreover, one small exothermic peak, corresponding to the formation of α-AlF_3, is observed around 973 K.

The DSC experiments of precursors P9−P12 (Figure 6) reveal three endothermic peaks which correspond to the transformation of β-$AlF_3 \cdot 3H_2O$ into α-AlF_3. The first of these, at 373 K, corresponds to the initial loss of water, probably due to sample moisture. The second and larger endothermic peak, at a temperature around 453 K, corresponds to the formation of ϵ_2-AlF_3 ($AlF_3 \cdot 0.5H_2O$). This peak is accompanied by a shoulder, detected around 420 K, which could be assigned to the formation of an intermediate such as ϵ_1-AlF_3 ($AlF_3 \cdot 1.5H_2O$), which has been previously reported by Wada et al.[13] The third peak, detected between 500 and 700 K, corresponds to a slow loss of the remaining water of the ϵ_2-AlF_3 structure to form α-AlF_3. The results obtained with DSC agree with X-ray diffraction and thermogravimetric analysis.

Scanning Electron Microscopy (SEM). The electron micrographs obtained from the precursors P1 (NH_4AlF_4), P8 ($(NH_4)_3AlF_6$), and P10 (β-$AlF_3 \cdot 3H_2O$) are shown in Figure 7. The micrographs reveal different morphologies for each sample. Precursor P1 (Figure 7a) shows a layered structure which agrees with the crystal structure described by Shinn et al.,[10] in which NH_4AlF_4 is formed by layers of AlF_6 octahedra joined by shared corners, and layers of NH_4^+ would lie between these layers. Precursor P8 (Figure 7b) shows a regular geometrical structure formed by large crystal particles around 25 mm in diameter that forms a truncated octahedron. This also agrees with the structure reported by Pauling,[22] in which $(NH_4)_3AlF_6$ is formed by a regular octahedron of fluorine atoms about each aluminum, with the octahedra being distributed in the positions of a face-centered-cubic lattice. On the other hand, precursor P10 (Figure 7c) shows an amorphous structure with greater porosity than the others, so the BET area of this sample (S10) is higher after calcination.

The micrographs of samples S1 and S8, both γ-AlF_3, (Figure 7d) reveal a layered structure for both samples. This agrees with the crystal structure described by Shinn et al.[10] in which γ-AlF_3 is formed by layers of planar sharing corners AlF_4 groups, and each aluminum atom is connected to a single unshared fluorine. These

(22) Pauling, L. *J. Am. Chem. Soc.* **1924**, *46*, 2738.

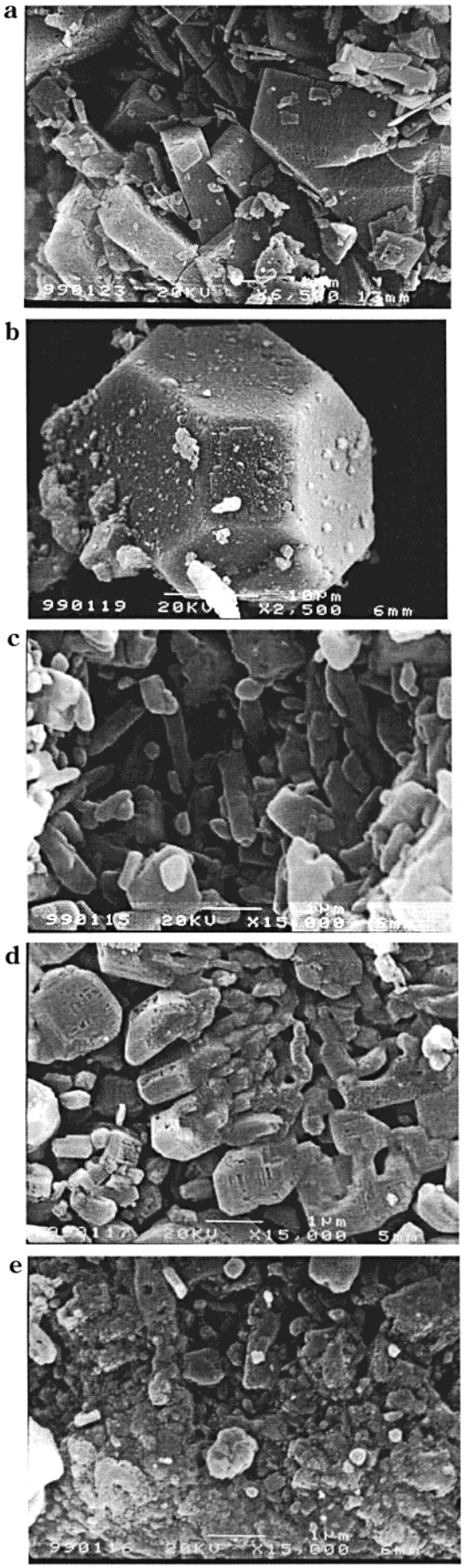

Figure 7. Scanning electron microscopy of (a) P1−P5, (b) P6−P8, (c) P9−P12, (d) S1−S8, (e) S9−S12.

results conclude that when $(NH_4)_3AlF_6$ decomposes on heating, with an initial loss of 2 mol of ammonium fluoride, ammonium tetrafluoroaluminate, which has a layered structure, is formed. Further heating results in the gradual loss of ammonium fluoride, and the final product is γ-AlF_3, which maintains the layered structure of the NH_4AlF_4 precursor. The micrograph of sample S10 (α-AlF_3) (Figure 7e) reveals an amorphous structure with high porosity that maintains the structure of the precursor P10 (β-$AlF_3 \cdot 3H_2O$).

BET Areas. The results of BET surface area determination for the samples are shown in Table 1. The BET surface areas of samples S9−S12 (α-AlF_3 phase), synthesized by thermal decomposition of precursors P9−P12 (β-$AlF_3 \cdot 3H_2O$), are between 71 and 123.5 m^2/g. These BET area values are 10−40 times larger than the one obtained by Herron[7] and Kemnitz et al.,[16] for the α-AlF_3 phase. These α-AlF_3 phases reported in the literature[8,10] were obtained by heating β-AlF_3 at 723 K and by passing gaseous hydrogen fluoride over anhydrous aluminum chloride at 1073 K. The synthetic strategies at high temperature implies low surface areas. The procedures proposed in this work are based on the synthesis of a precursor β-$AlF_3 \cdot 3H_2O$, which has a porous structure. The calcination of this precursor at 623 K implies the elimination of three molecules of water and the maintenance of the porous structure of the precursor, which yields to a high BET surface area for α-AlF_3.

The BET surface areas of the samples S1−S8 (γ-AlF_3 phase) range between 16 and 30 m^2/g. The BET surface area of sample S4 is smaller than 1 m^2/g because the precipitation was performed under high supersaturation conditions since ethanol was used in the synthesis of its precursor (P4). Data for the γ-AlF_3 surface area were not available in the revised literature. The synthesis of γ-AlF_3 implies the calcination of NH_4AlF_4 at 673 K. NH_4F (1 mol) escapes from the laminar structure of NH_4AlF_4 to form γ-AlF_3, which maintains the porosity and the laminar structure of its precursor. As it can be seen from the results, the synthetic strategies play an important role in obtaining high BET surface areas.

Conclusions

Different precursors of AlF_3 were synthesized by aqueous chemistry. NH_4AlF_4 and $(NH_4)_3AlF_6$ were the precursors of γ-AlF_3, and β-$AlF_3 \cdot 3H_2O$ was the precursor of α-AlF_3. These precursors and the samples were structurally characterized by X-ray diffraction, X-ray fluorescence, scanning electron microscopy, and infrared spectra. The transition of $(NH_4)_3AlF_6$ and NH_4AlF_4 to γ-AlF_3 and the transition of β-$AlF_3 \cdot 3H_2O$ to α-AlF_3 were studied by thermogravimetric analysis, temperature X-ray diffraction, and differential scanning calorimetry. These techniques conclude that $(NH_4)_3AlF_6$ decomposes at temperatures of around 500 K with an initial loss of 2 mol of NH_4F to form NH_4AlF_4. Further heating of ammonium tetrafluoroaluminate to 623 K results in the gradual loss of 1 mol of ammonium fluoride to form γ-AlF_3. At temperatures above 873 K, the metastable phase γ-AlF_3 irreversibly transforms to α-AlF_3, which is the most thermodynamically stable phase of aluminum fluoride. β-$AlF_3 \cdot 3H_2O$ thermally decomposes at temperatures of around 473 K with an initial loss of 2.5

mol of water to form a poor crystalline phase of aluminum fluoride named ϵ_2-AlF_3 ($AlF_3 \cdot 0.5H_2O$). This transforms to α-AlF_3 at temperatures above 573 K.

The BET area values of the materials obtained by calcination of the precursors are between 71−101 and 16−30 m^2/g for the α- and γ-AlF_3 phases, respectively. These values are much higher than those reported in the literature. These results suggest that our experimental procedures produce almost pure aluminum fluoride phases that show high BET areas with potential interest as catalysts or supports for fluorination reactions.

Acknowledgment. The authors are grateful for the financial support of the Ministerio de Educación y Cultura (AMB98-0545), the Generalitat de Catalunya (ACI 97), and Kal y Sol Iberia S.A.

CM991195G